

Synthesis, Spectroscopy Studies, and Theoretical Calculations of New Fluorescent Probes Based on Pyrazole Containing Porphyrins for Zn(II), Cd(II), and Hg(II) Optical Detection

Nuno M. M. Moura,^{†,‡,§} Cristina Núñez,^{‡,||,⊥} Sérgio M. Santos,[#] M. Amparo F. Faustino,[†] José A. S. Cavaleiro,[†] M. Graça P. M. S. Neves,^{*,†} José Luis Capelo,^{‡,§} and Carlos Lodeiro^{*,‡,§}

[†]Department of Chemistry and QOPNA, University of Aveiro, 3810-193 Aveiro, Portugal

[‡]BIOSCOPE Group, REQUIMTE-CQFB, Chemistry Department, Faculty of Science and Technology, University NOVA of Lisbon, 2829-516 Caparica, Portugal

[§]ProteoMass Scientific Society, Madan Park, Rua dos Inventores, 2825-182, Caparica, Portugal

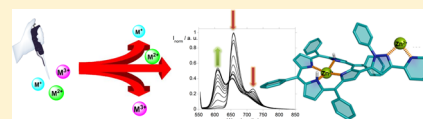
^{||}Department of Geographical and Life Sciences, Canterbury Christ Church University, CT1 1QU Canterbury, United Kingdom

[⊥]Inorganic Chemistry Department, Faculty of Chemistry, University of Santiago de Compostela, 15782 Santiago de Compostela, Spain

[#]Department of Chemistry and CICECO, University of Aveiro, 3810-193 Aveiro, Portugal

S Supporting Information

ABSTRACT: New pyrazole–porphyrin conjugates were successfully prepared from a reaction of β -porphyrin–chalcone derivatives with phenylhydrazine in acetic acid followed by an oxidative step. This fast and efficient synthetic approach provided the expected compounds in yields up to 82%. The sensing ability of the new porphyrin–pyrazole derivatives to detect the metal ions Ag^+ , Na^+ , K^+ , Mg^{2+} , Ca^{2+} , Ni^{2+} , Cu^{2+} , Zn^{2+} , Cd^{2+} , Hg^{2+} , Pb^{2+} , and Cr^{3+} was studied by spectrophotometric and spectrofluorimetric titrations. In the presence of Zn^{2+} , the conjugates exhibit changes in the emission spectra that are desired for a ratiometric-type fluoroionophoric detection probe. The studies were extended to gas phase, where the pyrazole–porphyrin conjugates show ability to sense metal ions with high selectivity toward Cu^{2+} and Ag^+ , and in poly(methyl methacrylate) doped films with promising results for Zn^{2+} detection.



INTRODUCTION

In recent years, the design and synthesis of new optical probes to be used in the recognition and sensing of a wide range of analytes have emerged as a research area of considerable importance.¹ In fact, the selection of spectrophotometric and spectrofluorimetric measurements as analytical tools has obvious advantages when compared with other alternatives due to the low cost, versatility, and accessibility of the techniques associated.²

The molecular devices converting metal ion recognition in physical recordable signals are continuously growing. Typically, chemosensors are molecules of abiotic origin that are able to selectively and reversibly bind the analyte. The main issue in the design of any effective chemosensor is the association of a selective molecular recognition event with a concomitant change in one or more properties of the system, such as absorption or fluorescence spectra.^{3,4} Changes in both the absorption and emission of light can be utilized as signals to detect and quantify some ions, working as chromophores and fluorophores (dual probe).^{4,5} The criteria for these probes are (i) stability, (ii) metal selectivity, (iii) metal affinity, (iv) signal transduction, (v) fluorescent signaling, (vi) kinetically rapid sensitization, and (vii) availability.⁶

Charged or neutral receptors bearing pyrrole, pyrazole, amide, or imidazolium moieties have been used in anion

recognition via H-bonding or via deprotonation of the NH in the receptor.⁷ Recently, pyrazole based compounds due to their metal coordination ability have been used as molecular detection probes of metal ions, such as Zn^{2+} , Cd^{2+} , and Hg^{2+} .⁸

Monitoring soft metal ions such as zinc(II) and copper(II) is of particular interest due to their well-known significant biological functions.^{9,10} Additionally, the high toxicity for living organisms of heavy metals like mercury(II) and cadmium(II) makes their detection also a subject of high relevance.^{11,12}

Porphyrins and related macrocycles exhibit interesting features, such as large Stokes shifts and relatively long excitation (>400 nm) and emission (>600 nm) wavelengths, to be used as fluorescent probes.^{13,14} In fact, several studies show that porphyrinic derivatives adequately functionalized in *meso*-positions are excellent candidates to be used in the detection of metal ions such as Zn^{2+} , Cd^{2+} , Hg^{2+} , or Pb^{2+} .¹⁵ However, most of the work using porphyrins as molecular probes in the detection of metal ions is based on macrocycles functionalized with adequate binding units in *meso*-positions, and as far as we know, much less attention is being given to β -functionalized porphyrins.¹⁶

Received: March 19, 2014

Published: June 3, 2014

Pyrazole derivatives are well known five membered heterocycles with a broad spectrum of promising biological activity, namely, as anticancer agents.¹⁷ Furthermore, pyrazoles are recognized as important motifs to be used as ligands in coordination chemistry, as building blocks in heterocyclic synthesis, as optical brighteners, and UV stabilizers, and also as units to construct supramolecular and photoinduced electron-transfer systems.¹⁸

Recently, we described an efficient access to porphyrin-pyrazoline and porphyrin-pyrazole derivatives via 1,3-dipolar cycloaddition reactions involving *N*-aryl-*C*-ethoxycarbonylnitrile imines, generated *in situ* by base-induced dehydrobromination of ethyl hydrazono- α -bromoglyoxylates and 2-vinyl-5,10,15,20-tetraphenylporphyrin.¹⁹ Following our interest in β -functionalization of *meso*-tetraarylporphyrins,²⁰ namely, via the formyl group,²¹ and considering that the conjugation of these tetrapyrrolic macrocycles to pyrazoline/pyrazole entities could potentiate their sensorial ability, we decided to consider here a more conventional strategy²² to introduce those heterocyclic moieties in the porphyrin core: the reaction of porphyrins bearing chalcone units with hydrazine derivatives.

In this Article, we report an efficient synthesis of new pyrazole-porphyrin conjugates, the photophysical characterization of these ligands, and also their coordination interaction with metal ions via sensorial response to different metals in solution, solid supports, and gas phase.

■ EXPERIMENTAL SECTION

General Remarks. ¹H and ¹³C solution NMR spectra were recorded on Bruker Avance 300 (300.13 and 75.47 MHz, respectively) and 500 (500.13 and 125.76 MHz, respectively) spectrometers. CDCl₃ was used as solvent and tetramethylsilane (TMS) as internal reference; the chemical shifts are expressed in δ (ppm) and the coupling constants (*J*) in Hertz (Hz).

Unequivocal ¹H assignments were made using 2D COSY (¹H/¹H), while ¹³C assignments were made on the basis of 2D HSQC (¹H/¹³C) and HMBC (delay for long-range *J* C/H couplings were optimized for 7 Hz) experiments. Mass spectra were recorded using MALDI TOF/TOF 4800 Analyzer (Applied Biosystems MDS Sciex), with CHCl₃ as solvent and without a matrix. Mass spectra HRMS were recorded on an APEXQe FT-ICR (Bruker Daltonics, Billerica, MA) mass spectrometer using CHCl₃ as solvent; in *m/z* (rel. %). The UV-vis spectra were recorded on an UV-2501 PC Shimadzu spectrophotometer using CHCl₃ as solvent. Preparative thin-layer chromatography was carried out on 20 × 20 cm glass plates coated with silica gel (0.5 mm thick). Column chromatography was carried out using silica gel (Merck, 35–70 mesh). Analytical TLC was carried out on precoated sheets with silica gel (Merck 60, 0.2 mm thick).

All of the chemicals were used as supplied. Solvents were purified or dried according to the literature procedures.²³

Chemicals and Starting Reagents. AgBF₄·xH₂O, NaBF₄, KBF₄, Mg(OTf)₂, Ca(BF₄)₂·xH₂O, Ni(BF₄)₂·xH₂O, Cu(BF₄)₂·6H₂O, Zn(BF₄)₂·xH₂O, Cd(CF₃SO₃)₂·xH₂O, Hg(CF₃SO₃)₂·xH₂O, Pb(OTf)₂, and Cr(NO₃)₃·xH₂O were purchased from Strem Chemicals, Sigma-Aldrich, or Solchemar. All of these chemicals were used without further purification. The solvents were obtained from Panreac and Riedel-de-Haën and were used as received or distilled and dried using standard procedures.

Synthesis of the Porphyrinic Precursors. The porphyrin-chalcone type derivatives **1a–d** were prepared from 2-formyl-5,10,15,20-tetraphenylporphyrin²⁴ and aryl methyl ketones in the presence of piperidine and catalytic amounts of La(OTf)₃ in dry toluene, according to a literature procedure.²⁵

General Procedure for the Synthesis of the Organic Ligands. A solution of the appropriate porphyrin-chalcone **1a–d** (25.0 mg) in CHCl₃/MeOH (3:1) was stirred in the presence of Cu(OAc)₂·H₂O (1.5 equiv) for 30 min at 50 °C. The reaction was followed by UV/vis

until total consumption of the starting porphyrin. After cooling, the reaction mixture was washed with water and extracted with dichloromethane. The organic phase was dried (Na₂SO₄), and the solvent was evaporated under reduced pressure. The resulting residues were crystallized from CH₂Cl₂/hexane, and the desired compounds **2a–d** were obtained in quantitative yields.

Then, to the respective copper complex **2a–d** (20 mg) dissolved in acetic acid (2.0 mL), phenylhydrazine (1.5 equiv) was added, and the resulting mixture was maintained under stirring for 1 to 5 h at 120 °C (see Table 1). After the required period, the mixture was carefully neutralized with an ice-cold aqueous saturated solution of Na₂CO₃ until pH 7, and the reaction mixture was extracted in CH₂Cl₂. The organic layer was separated, dried (Na₂SO₄), and the solvent evaporated.

The crude obtained was dissolved in dry toluene (1.5 mL), and after adding *o*-chloranil (3 equiv), the resulting mixture was stirred for 1 h at 120 °C. After cooling, the reaction mixture was washed with water and extracted with dichloromethane. The organic phase was dried (Na₂SO₄), and the solvent was evaporated under reduced pressure.

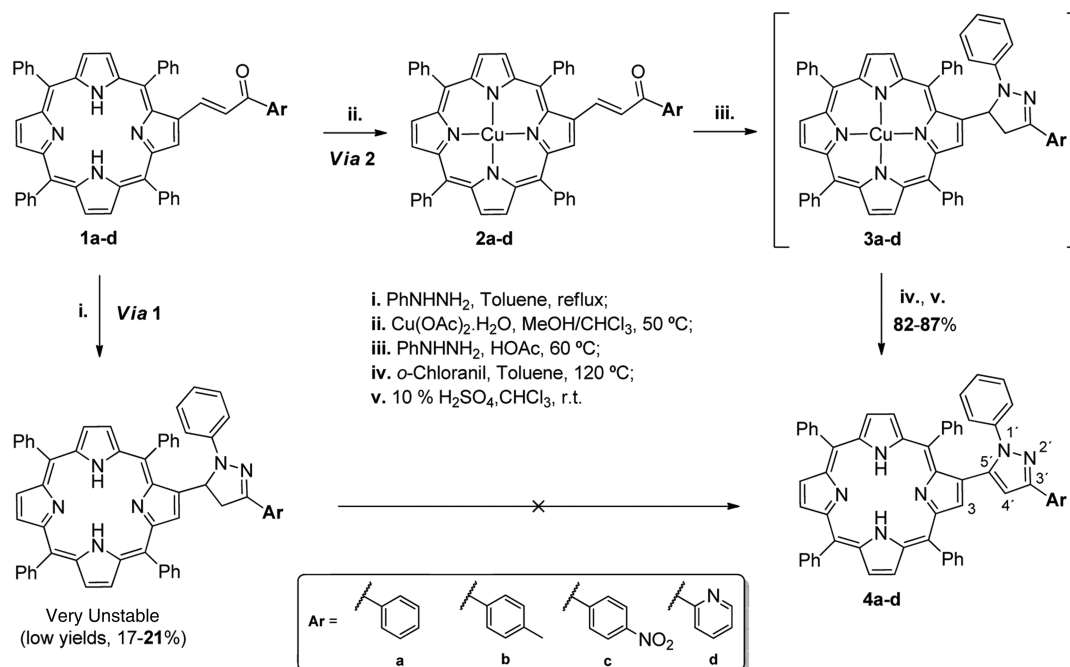
The resulting residue was stirred under vigorous agitation in a minimal amount of a 10% solution of H₂SO₄ in CHCl₃, at room temperature, for 15 min. The mixture was then carefully neutralized with an ice-cold aqueous saturated solution of Na₂CO₃ and then was extracted with CH₂Cl₂. The organic layer was separated and dried (Na₂SO₄), and the solvent was evaporated under vacuum. The residue was purified by column chromatography using CH₂Cl₂/petroleum ether (3:1) as the eluent. Compounds **4a–d** (see Table 1 for the yields) were obtained pure after crystallization from CH₂Cl₂/hexane. The fractions obtained were fully characterized by NMR, mass, and UV/vis techniques.

2-(1,3-Diphenyl-1H-pyrazol-5-yl)-5,10,15,20-tetraphenylporphyrin, 4a. ¹H NMR (300 MHz, CDCl₃): δ 8.87 (2H, d, *J* = 5.0 Hz, H- β), 8.82–8.77 (2H, m, H- β), 8.77 (1H, AB, *J* = 5.0 Hz, H- β), 8.70 (1H, s, H-3), 8.67 (1H, AB, *J* = 5.0 Hz, H- β), 8.23–8.18 (4H, m, H-*o*-Ph), 8.06 (2H, d, *J* = 6.9 Hz, H-*o*-Ph), 7.88 (2H, d, *J* = 6.9 Hz, H-*o*-Ph), 7.89–7.63 (11H, m, H-*m,p*-Ph, and H-2''',6'''), 7.49–7.45 (3H, m, H-3''',5''', and H-4'''), 7.39–7.32 (5H, m, H-Ph, and H-2'',6''), 6.93–6.89 (3H, m, H-3'',5'', and H-4''), 6.48 (1H, s, H-4'), –2.65 (2H, s, NH) ppm. ¹³C NMR (75 MHz, CDCl₃): δ 151.4, 142.02, 141.95, 141.7, 140.4, 140.1, 140.0, 134.7, 134.6, 134.5, 133.4, 133.1–129.9 (C- β), 128.5, 128.3, 128.0, 127.8, 127.6, 126.8, 126.7, 126.6, 126.1, 126.0, 125.9, 123.4, 120.9, 120.5, 120.3, 108.5 ppm. UV-vis (CHCl₃): λ_{max} (log ϵ) 423.0 (5.46), 519.0 (4.20), 555.0 (3.77), 594.0 (3.76), 651.0 (3.54) nm. MS (MALDI): *m/z* 833.3 [M + H]⁺. HRMS-ESI(+): *m/z* calculated to C₅₉H₄₁N₆ [M + H]⁺ 833.3387; found, 833.3392.

2-(1-Phenyl-3-(*p*-tolyl)-1H-pyrazol-5-yl)-5,10,15,20-tetraphenylporphyrin, 4b. ¹H NMR (300 MHz, CDCl₃): δ 8.87 (2H, AB, *J* = 4.9 Hz, H- β), 8.82–8.78 (2H, m, H- β), 8.76 (1H, AB, *J* = 4.9 Hz, H- β), 8.70 (1H, s, H-3), 8.67 (1H, AB, *J* = 4.9 Hz, H- β), 8.23–8.18 (4H, m, H-*o*-Ph), 8.06 (2H, d, *J* = 6.9 Hz, H-*o*-Ph), 7.87 (2H, d, *J* = 6.9 Hz, H-*o*-Ph), 7.80–7.61 (11H, m, H-*m,p*-Ph, and H-2''',6'''), 7.37–7.29 (7H, m, H-Ph, H-2'',6'', and H-3''',5'''), 6.92–6.86 (3H, m, H-3'',5'', and H-4''), 6.45 (1H, s, H-4'), 2.44 (3H, s, CH₃), –2.66 (2H, s, NH) ppm. ¹³C NMR (75 MHz, CDCl₃): δ 151.4, 142.03, 141.95, 141.7, 140.4, 140.1, 137.4, 134.7, 134.6, 134.5, 134.0–130.8 (C- β), 130.6, 129.2, 129.1, 128.3, 128.0, 127.81, 127.76, 126.8, 126.7, 126.6, 126.1, 125.9, 125.8, 123.4, 120.9, 120.5, 120.2, 108.3, 21.4 (CH₃) ppm. UV-vis (CHCl₃): λ_{max} (log ϵ) 423.0 (5.41), 520.0 (4.12), 555.0 (3.67), 594.0 (3.57), 650.0 (3.43) nm. MS (MALDI): *m/z* 847.3 [M + H]⁺. HRMS-ESI(+): *m/z* calculated to C₆₀H₄₃N₆ [M + H]⁺ 847.3544; found, 847.3553.

2-(1-Phenyl-3-(4-nitrophenyl)-1H-pyrazol-5-yl)-5,10,15,20-tetraphenylporphyrin, 4c. ¹H NMR (300 MHz, CDCl₃): δ 8.88 (2H, AB, *J* = 5.0 Hz, H- β), 8.82–8.79 (3H, m, H- β), 8.68–8.66 (2H, m, H- β), 8.32 (2H, AB, *J* = 8.9 Hz, H-3''',5'''), 8.23–8.18 (4H, m, H-*o*-Ph), 8.04 (2H, d, *J* = 7.3 Hz, H-*o*-Ph), 7.97 (2H, AB, *J* = 8.9 Hz, H-2''',6'''), 7.91 (2H, d, *J* = 7.3 Hz, H-*o*-Ph), 7.80–7.60 (9H, m, H-*m,p*-Ph), 7.38–7.28 (5H, m, H-*m,p*-Ph, and H-2'',6''), 6.99–6.90 (3H, m, H-3''',5'', and H-4''), 6.53 (1H, s, H-4'), –2.67 (2H, s, NH) ppm. ¹³C NMR (75 MHz, CDCl₃): δ 148.9, 147.0, 141.9, 141.9, 141.6, 140.9, 140.4, 140.0, 139.7,

Scheme 1



134.7, 134.6, 134.5, 134.1–129.8 (C- β), 128.6, 128.5, 127.9, 127.8, 126.8, 126.73, 126.65, 126.57, 126.0, 124.0, 123.6, 120.59, 120.56, 120.4, 108.9 ppm. UV–vis (CHCl₃): λ_{max} (log ϵ) 423.0 (5.40), 519.0 (4.15), 554.0 (3.69), 593.0 (3.62), 652.0 (3.52) nm. MS (MALDI): m/z 878.3 [M + H]⁺. HRMS-ESI(+): m/z calculated to C₅₉H₄₀N₇O₆ [M + H]⁺ 878.3238; found, 878.3239.

2-(1-Phenyl-3-(2-pyridyl)-1H-pyrazol-5-yl)-5,10,15,20-tetraphenylporphyrin, 4d. ¹H NMR (300 MHz, CDCl₃): δ 8.89 and 8.87 (2H, AB, J = 5.0 Hz, H- β), 8.82–8.78 (3H, m, H- β), 8.74 (1H, AB, J = 4.9 Hz, H- β), 8.71 (1H, ddd, J = 1.7 and 4.9 Hz, H-6''), 8.62 (1H, AB, J = 4.9 Hz, H- β), 8.23–8.17 (4H, m, H- α -Ph), 8.11 (2H, d, J = 7.0 Hz, H- α -Ph), 7.87 (1H, d, J = 7.9 Hz, H-3''), 7.82–7.67 (12H, m, H- α , m , p -Ph, and H-4''), 7.36–7.26 (6H, m, H-Ph, H-2'', 6'', and H-5''), 6.96 (1H, s, H-4'), 6.88–6.82 (3H, m, H-3'', 5'', and H-4''), –2.65 (2H, s, NH) ppm. ¹³C NMR (75 MHz, CDCl₃): δ 152.2, 151.4, 149.3, 142.0, 141.9, 141.7, 140.5, 140.3, 139.7, 136.5, 134.7, 134.6, 134.5, 132.6–139.7 (C- β), 128.2, 127.8, 127.8, 127.7, 126.8, 126.7, 126.2, 126.0, 123.2, 122.4, 121.0, 120.5, 120.4, 120.3, 120.2, 109.8 ppm. UV–vis (CHCl₃): λ_{max} (log ϵ) 423.0 (5.53), 520.0 (4.25), 554.0 (3.81), 594.0 (3.72), 650.0 (3.60) nm. MS (MALDI): m/z 834.3 [M + H]⁺. HRMS-ESI(+): m/z calculated to C₅₈H₄₀N₇ [M + H]⁺ 834.3340; found, 843.3336.

Physical Measurements. The MALDI-MS analyses were performed in a MALDI-TOF-TOF-MS model Ultraflex II (Bruker, Germany) equipped with nitrogen, from the BIOSCOPE group. Each spectrum represents accumulations of 5 × 50 laser shots. The reflection mode was used. The ion source and flight tube pressure were less than 1.80 × 10^{–7} and 5.60 × 10^{–8} Torr, respectively. The MALDI mass spectra of the soluble samples (1 or 2 μ g/ μ L) were recorded using the “dried droplet” and the “layer-by-layer” sample preparation methods. In both methods, the ligands were dissolved in chloroform and the metal salts in acetonitrile, but the introduction in the sample holder was different. In the dried-droplet method, the two solutions containing the ligand (1 μ L) and the metal salt (1 μ L) were mixed and then applied to the MALDI-TOF-MS sample holder. In the layer-by-layer method, a solution of each ligand was spotted in the MALDI-TOF plate and then dried; subsequently, 1 μ L of the solution containing the metal salt was placed on the sample holder, which was then inserted into the ion source. In this case, the chemical reaction between the ligand and the metal salts occurred in the holder, and the complex species were produced in gas phase.

Spectrophotometric and Spectrofluorimetric Measurements.

Absorption spectra were recorded on a JASCO V-650 spectrophotometer, and fluorescence emission spectra were recorded on a Horiba Jobin-Yvon Fluoromax 4 spectrofluorimeter. The linearity of the fluorescence emission versus the concentration was checked in the concentration range used (10^{–4}–10^{–6} M). The correction of the absorbed light was performed when it was considered necessary. The spectrophotometric characterizations and titrations were performed by preparing stock solutions of the compounds in chloroform (ca. 10^{–3} M) in a 10 mL volumetric flask. The studied solutions were prepared by appropriate dilution of the stock solutions up to 10^{–5}–10^{–6} M. Titrations of the probes (4a–d) were carried out by the addition of microliter amounts of standard solutions of the metal ions in acetonitrile in a 1 cm quartz cell. All of the measurements were performed at 298 K.

Luminescence quantum yields of compounds 4a–d were measured using a solution of crystal violet in methanol as standard ([Φ] = 0.54),²⁶ and all values were corrected taking into account the solvent refractions index. Fluorescence spectra of solid samples were recorded using a fiber optic system connected to a Horiba Jobin-Yvon Fluoromax 4 spectrofluorimetric excited at appropriated λ (nm) of the solid compounds.

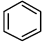
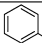
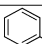
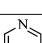
Preparation of PMMA Polymer Films Doped with Compound 4a. The preparation of the poly(methyl methacrylate) (PMMA) film was performed by dissolving the PMMA powder (100 mg) in chloroform, followed by the addition of ligand 4a (1–5 mg) dissolved in the same solvent. The polymer film was obtained after evaporation of solvent at 40 °C under vacuum for 24 h.^{27,28} Because of the spectroscopic characteristics, the film doped with 5 mg of the ligand was selected for the studies with the metal ions.

Theoretical Studies. Theoretical calculations were performed using density functional theory with the B3LYP functional and the LanL2DZ basis set using Gaussian 09.²⁹ Default parameters were used in all geometry optimizations.

RESULTS AND DISCUSSION

Synthesis. The new pyrazole–porphyrin conjugates 4a–d were synthesized as outlined in Scheme 1. The starting porphyrin-chalcone derivatives 1a–d were prepared from the condensation of 2-formyl-5,10,15,20-tetraphenylporphyrin²⁴ with the adequate aryl methyl ketone using piperidine as base

Table 1. Reaction Times and Overall Yields Obtained in the Synthesis of Compounds 4a–d

Entry	Ar	Time (h) ^a				4 η (%)
		i.	ii.	iii.	iv.	
1			3			84
2			3			86
4		0.5	5	1	0.5	82
5			1			87

^a i., complexation; ii., condensation with phenylhydrazine; iii., oxidation; and iv., descomplexation.

Table 2. Photophysical Data of Compounds 4a–d in CHCl₃ and in Solid State at 298 K

compd	λ_{max} (nm)/log ϵ	λ_{em} (nm)	Stokes shift (nm)	Φ_{Flu}	λ_{em} (nm) _{solid}
4a	423:5.46	658, 719	7	0.02	668, 737, 822
	519:4.20				
	555:3.77				
	594:3.76				
	651:3.54				
4b	423:5.41	660, 719	10	0.02	667, 732, 819
	520:4.12				
	555:3.67				
	594:3.57				
	650:3.43				
4c	423:5.40	659, 720	7	0.02	669, 738, 821
	519:4.15				
	554:3.69				
	593:3.62				
	652:3.52				
4d	423:5.53	660, 719	10	0.02	673, 731, 821
	520:4.25				
	554:3.81				
	594:3.72				
	650:3.60				

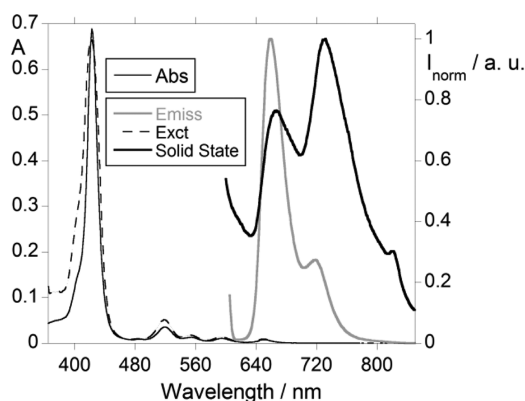


Figure 1. Absorption and normalized emission and excitation of chemosensor 4b in CHCl₃ ([4b] = 2.50×10^{-6} M, $\lambda_{\text{exc}4b}$ = 601 nm, and $\lambda_{\text{emiss}4b}$ = 728 nm) and emission of spectra in solid state at room temperature.

in the presence of catalytic amounts of La(OTf)₃ according to the literature.²⁵

In the first attempts to obtain 4a–d, we tried to perform the reaction using the free-base chalcones 1a–d and phenylhydrazine. The condensation was done in refluxing toluene, and after 48 h of reaction, we were able to isolate the respective porphyrin-pyrazoline derivative but in very low yields (~20%) and accompanied by an appreciable amount of the starting porphyrin (~75%). However, these pyrazoline derivatives were highly unstable when subjected to chromatography and even when kept under storage (Scheme 1, via 1). This fact prompts us to modify the approach having in mind that the condensation conditions must be improved and that we must proceed directly to pyrazole–porphyrin conjugates without purification of the pyrazoline intermediates (Scheme 1, via 2).

In an attempt to find better conditions for the reaction and based on literature,³⁰ we decided to use acetic acid as solvent. We found that in this medium, the condensation of phenylhydrazine with the free base porphyrins 1a–d did not occur and that the starting porphyrin was fully recovered. Therefore, in order to avoid the protonation of the inner core of the macrocycle by the acidic medium, probably responsible for the unsuccessful condensation with the free bases, we decided to prepare the copper(II) complexes 2a–d following the typical procedure described in the literature to introduce this metal in porphyrins.³¹ After this key step, the reactions of chalcones 2a–d with phenylhydrazine were performed at 60 °C, and after 1 to 5 h, depending on the porphyrin derivative used, the reaction's TLC revealed the absence of starting metalloporphyrin 2a–d and the formation in all cases of only one new product, the porphyrin-pyrazoline derivative 3a–d. Then, the resulting crude obtained after workup was dissolved in toluene, and refluxed for 1 h in the presence of *o*-chloranil (3 equiv). After this period, TLC monitoring revealed the total consumption of the starting substrate and the formation of a new more polar compound, which was then treated with 10% H₂SO₄ conc/CHCl₃ in order to remove the paramagnetic metal. After workup and column chromatography (silica gel), the pyrazole–porphyrin conjugates 4a–d were isolated in yields between 82% and 87% (see in Table 1 the yields of the compounds 4a–d obtained after optimization of the reaction conditions).

The structures of all conjugates were unambiguously confirmed by spectroscopic data, namely, NMR, UV–vis, and mass spectroscopy techniques.

The ¹H NMR spectra of the pyrazole–porphyrin conjugates 4a–d are consistent with β -substituted porphyrins showing the resonance of the corresponding H-3 as a singlet at ca. 8.7 ppm. The hydrogens of the *meso*-phenyl groups appear as multiplets between ca. 7.6 and 8.2 ppm, while the proton resonances of the aryl group at position 3 in the pyrazole unit appear with the expected AB pattern for compounds 4a and 4c. In the particular case of compound 4d, the attribution of the signals generated by the resonance of the hydrogens in the pyridine ring were done using 2D COSY experiments. The resonances of the *N*-phenyl group hydrogens appear as two multiplets in ranges of 6.8–7.0 and 7.2–7.4 ppm.

Considering the resonances of the pyrazole moiety hydrogens, the most important features are the presence of a characteristic signal at ca. 6.5 ppm due to the resonance of hydrogen H-4'. As expected, the singlets generated by the inner pyrrolic hydrogens appear around –2.65 ppm.

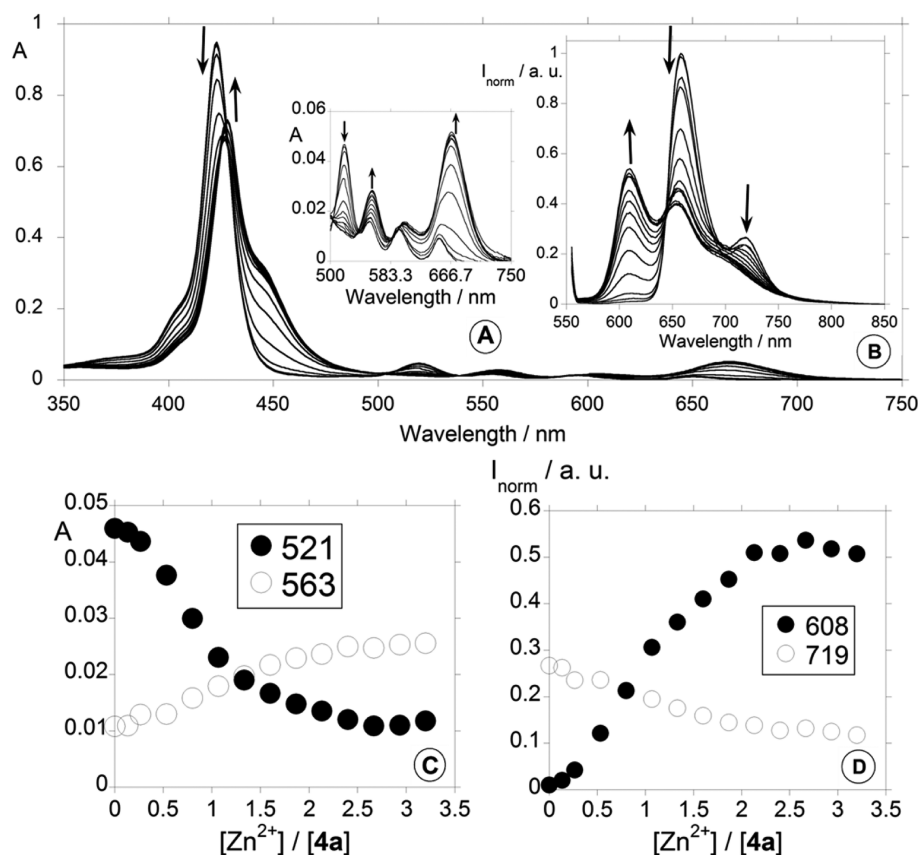


Figure 2. Spectrophotometric (A) and spectrofluorimetric (B) titrations of compound **4a** in chloroform as a function of added Zn^{2+} in acetonitrile. The inset shows the partial absorption spectra between 500 and 750 nm (A). (C) Absorption at 521 and 563 nm and (D) the normalized fluorescence intensity at 608 and 719 nm (B) ($[\text{4a}] = 2.50 \times 10^{-6}$ M, and $\lambda_{\text{exc4a}} = 539$ nm).

Table 3. Stability Constants and Stoichiometry for Chemosensors **4a–d in CHCl_3 in the Presence of Zn^{2+} , Hg^{2+} , Cd^{2+} , and Cu^{2+}**

compd	interaction (M/L)	$\Sigma \log \beta$ (Abs)	$\Sigma \log \beta$ (emiss)
4a	Zn^{2+} (1:2)	$13.10 \pm 2.38 \times 10^{-3}$	$12.76 \pm 7.38 \times 10^{-3}$
	Hg^{2+} (1:2)	$13.34 \pm 3.53 \times 10^{-3}$	$13.71 \pm 2.22 \times 10^{-2}$
	Cd^{2+} (1:2)	$12.40 \pm 1.04 \times 10^{-3}$	$12.36 \pm 8.45 \times 10^{-3}$
	Cu^{2+} (1:2)	$11.91 \pm 2.59 \times 10^{-3}$	$12.49 \pm 3.05 \times 10^{-3}$
4b	Zn^{2+} (1:2)	$11.28 \pm 4.67 \times 10^{-3}$	$10.39 \pm 4.96 \times 10^{-2}$
	Hg^{2+} (1:2)	$11.71 \pm 2.10 \times 10^{-3}$	$11.71 \pm 2.10 \times 10^{-3}$
	Cd^{2+} (1:2)	$11.35 \pm 1.37 \times 10^{-3}$	$11.35 \pm 1.37 \times 10^{-3}$
	Cu^{2+} (1:2)	$13.26 \pm 1.52 \times 10^{-3}$	$13.26 \pm 1.52 \times 10^{-3}$
4c	Zn^{2+} (1:2)	$12.30 \pm 2.99 \times 10^{-3}$	$12.30 \pm 2.99 \times 10^{-3}$
	Hg^{2+} (1:2)	$13.29 \pm 2.01 \times 10^{-3}$	$13.29 \pm 2.01 \times 10^{-3}$
	Cd^{2+} (1:2)	$12.42 \pm 1.34 \times 10^{-3}$	$11.15 \pm 1.66 \times 10^{-2}$
	Cu^{2+} (1:2)	$12.40 \pm 1.81 \times 10^{-3}$	$13.11 \pm 2.36 \times 10^{-2}$
4d	Zn^{2+} (2:1)	$11.94 \pm 2.03 \times 10^{-3}$	$11.94 \pm 2.03 \times 10^{-3}$
	Hg^{2+} (2:1)	$12.04 \pm 2.61 \times 10^{-3}$	$12.14 \pm 1.13 \times 10^{-2}$
	Cd^{2+} (2:1)	$11.25 \pm 2.93 \times 10^{-3}$	$10.55 \pm 1.57 \times 10^{-2}$
	Cu^{2+} (2:1)	$12.77 \pm 2.27 \times 10^{-3}$	$13.15 \pm 8.56 \times 10^{-3}$

Photophysical Characterization. The photophysical characterization of compounds **4a–d** was performed in chloroform solution at 298 K, and the main photophysical data are summarized in Table 2. In Figure 1 is shown the absorption, excitation, and emission spectra of compound **4b** as an example of the pyrazole–porphyrin conjugates (see also Figure S12 in Supporting Information for compounds **4a**, **4c**,

and **4d**). In the same figure is also shown the emission spectra obtained from the solid state of the same derivative.

The absorption spectra of porphyrin–pyrazole type derivatives **4a–d** show the typical features of free base porphyrins due to $\pi-\pi^*$ transitions: the highly intense Soret band at 423 nm and the four well-defined Q bands with decreased intensity between 519 and 652 nm. The perfect match between the absorption and the excitation spectra rules out the presence of any emissive impurity.

The fluorescence emission spectra of compounds **4a–d** obtained after excitation at ca. 595 nm present two bands centered at ca. 660 and 720 nm that are characteristic of porphyrin derivatives (see Figure 1) and where the first vibrational mode of the fluorescence is more pronounced. The porphyrin–pyrazole type derivatives **4a–e** showed Stokes shifts between 7 and 10 nm. The fluorescence quantum yields (Φ_{Flu}), determined by the internal reference method with respect to a solution of crystal violet in methanol as a standard ($[\Phi_{\text{Flu}}] = 0.54$),²⁶ are shown in Table 2. The values of fluorescence quantum yields for compounds **4a–d** were 0.02. Compounds **4a–d** presented lower relative fluorescence quantum yields (0.02) than the related free base porphyrins (Φ_{Flu} of TPP = 0.11). The low fluorescence efficiency of this type of molecules can probably be attributed to an alteration of the planarity of the porphyrin core, due to the presence of the extra chain that can be responsible by a more reduced π -electron mobility.³²

The emission spectra of the solid powder of ligands **4a–d** were also measured, using a fiber optic system connected to the Horiba Jobin-Yvon Fluoromax 4 (Table 2 and Figure 1). These

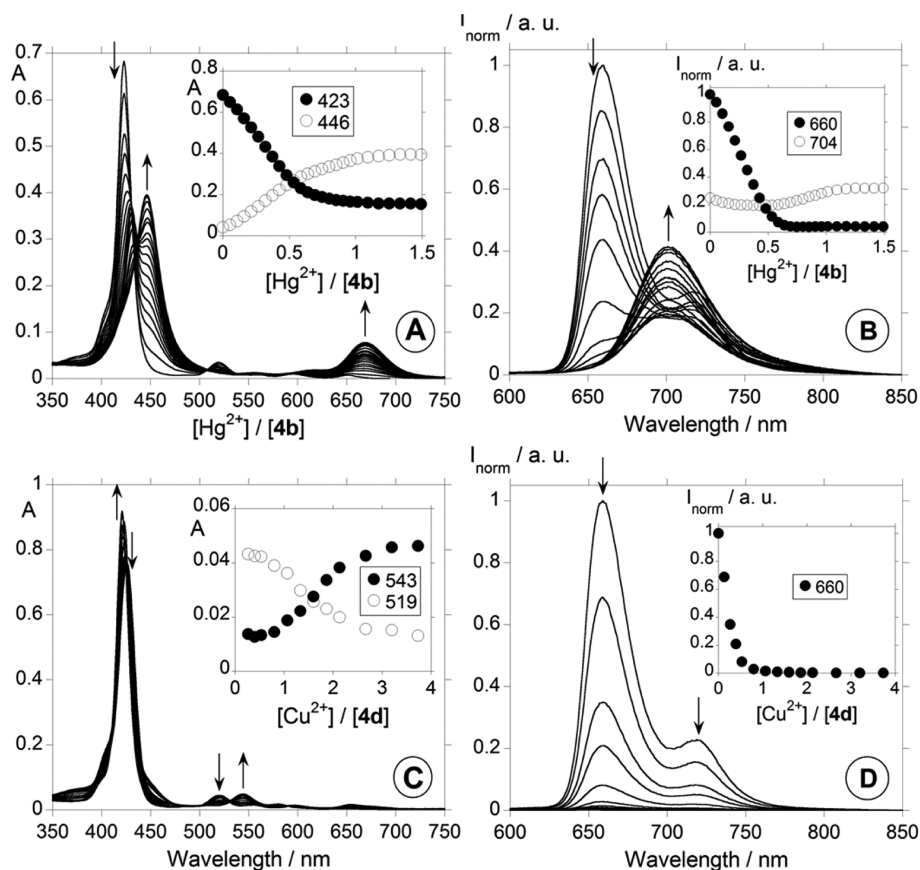


Figure 3. Spectrophotometric (A and C) and spectrofluorimetric (B and D) titrations of conjugates **4b** and **4d** in chloroform as a function of added Hg^{2+} and Cu^{2+} , respectively, in acetonitrile. The insets show the absorption at 423 and 446 nm (A) and at 519 and 543 nm (C); and the normalized fluorescence intensity at 660 and 704 (B) and at 660 nm (D) ($[\text{4b}] = [\text{4d}] = 2.50 \times 10^{-6} \text{ M}$, $\lambda_{\text{exc4b}} = \lambda_{\text{exc4d}} = 338 \text{ nm}$).

solid state spectra show fluorescence bands between 667 and 822 nm with maximum intensities different from the ones observed in solution.

Metal Binding Studies. The sensorial ability of conjugates **4a–d** toward the different charged metal ions Ag^+ , Na^+ , K^+ , Mg^{2+} , Ca^{2+} , Ni^{2+} , Cu^{2+} , Zn^{2+} , Cd^{2+} , Hg^{2+} , Pb^{2+} , and Cr^{3+} was investigated by the titration of the ligands, dissolved in chloroform, with small amounts of the adequate metal salt dissolved in acetonitrile. These experiments were followed by UV/vis and fluorescence emission spectroscopy and were performed at 25°C . No changes were detected for compounds **4a–d** when titrated with the metal ions Na^+ , K^+ , Ca^{2+} , Mg^{2+} , Pb^{2+} , Ni^{2+} , Ag^+ , and Cr^{3+} . The most significant changes in the ground and excited states were observed in the presence of Cu^{2+} , Zn^{2+} , Cd^{2+} , and Hg^{2+} .

The titration of compounds **4a–d** with Zn^{2+} induces significant changes in the absorption spectra with a small bathochromic shift ($\sim 5 \text{ nm}$) of the initial Soret band. These changes in the Soret band region are accompanied by a decrease of the Q-band at ca. 520 nm, a small increase of the band centered at ca. 555 nm, and by the formation of a new band at 660 nm (Figure 2A). These changes in the absorption spectra suggest the binding of the metal ion to the nitrogen atoms in the inner core of the porphyrinic macrocycle without deprotonation.³³

Meanwhile, a significant change also occurs in the fluorescent emission spectrum of pyrazole–porphyrin conjugates **4a–d** after the addition of Zn^{2+} , as is exemplified in Figure 2B for compound **4a**. The fluorescent emission intensity of this

conjugate at 659 nm decreases significantly, while a new fluorescent emission peak appears at 608 nm, leading to a significant change in the ratio of F_{608}/F_{659} . This new emission band, which increases with the addition of Zn^{2+} , can be assigned to a metal-to-ligand charge transfer and indicates the generation of a new fluorophore arising from the metal–porphyrin association. Compounds **4b–d** show spectral behavior similar to the one described for compound **4a** after titration with Zn^{2+} .

The association constants for the interaction of Zn^{2+} with the different ligands were determined using the HypSpec³⁴ program and are summarized in Table 3. The results from the titrations of conjugates **4a–d** with Zn^{2+} suggest complex formation in a stoichiometry of one metal ion per two ligands ($\text{M/L} = 1:2$), with ligands **4a–c**, and two metals per ligand ($\text{M/L} = 2:1$), for ligand **4d**. The binding modes between ligands **4a–d** and Zn^{2+} are shown in Figures 6 and 7 (see the Theoretical Calculations section).

Therefore, compounds **4a–d** exhibit changes in the emission spectra upon the binding of the Zn^{2+} ion typical for a ratiometric-type fluorionophoric probe.

The titration of ligands **4a–d** with Hg^{2+} shows alterations similar to the ones observed in the presence of Zn^{2+} but with a more prominent red shift of the Soret band from 423 to 448 nm. This shift is accompanied by the formation of a new band at ca. 670 nm and a drastic decrease of the four initial Q bands centered between 520 and 652 nm; two well-defined isosbestic points were observed at ca. 438 and 510 nm (see Figure 3A).

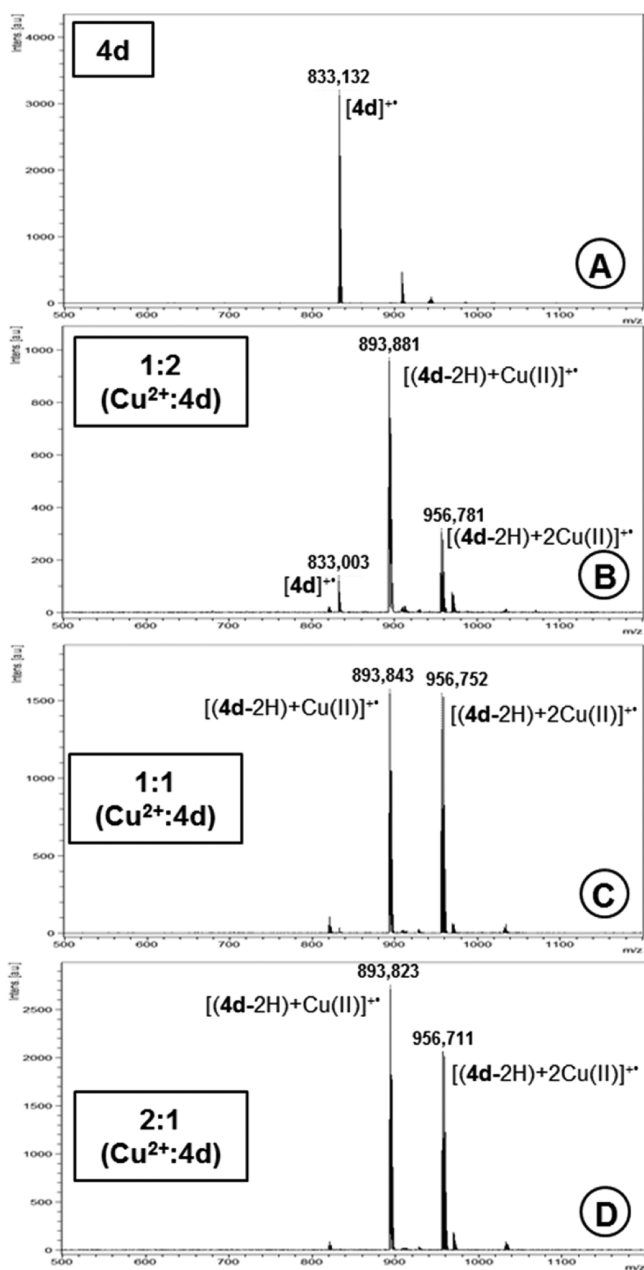


Figure 4. MALDI-TOF mass spectra of compound **4d** before (A) and after titration with 0.5 (B), 1.0 (C), and 2.0 (D) equiv of $\text{Cu}(\text{BF}_4)_2 \cdot 6\text{H}_2\text{O}$ using the layer-by-layer deposition method.

In the excited state, upon the addition of Hg^{2+} aliquots to pyrazole–porphyrin conjugates **4a** and **4b** a decrease in the emission intensity of the two initial bands centered at ca. 660 and 719 nm followed by the formation of a new band at 704 nm (Figure 3B) was observed. It is worth noting that usually the Hg^{2+} ion acts as a fluorescence quencher via a spin–orbital coupling effect.³⁵ In fact, this was the behavior of ligands **4c** and **4d** upon binding with Hg^{2+} where a quenching of the two initial bands was detected. The stability constants for the interaction of compounds **4a–d** with Hg^{2+} and the stoichiometry of the complexes are summarized in Table 3.

When compounds **4a–d** were titrated with Cd^{2+} , the spectral changes in the ground state were analogous to the ones described in the titrations with the previous metal ions. In the excited state, a pronounced quenching (~55%) in the emission

intensity in the presence of this metal for all conjugates was detected.

The addition of Cu^{2+} to conjugates **4a–d** induces in the first part of the titration, a decrease in the Soret band and in the Q-band centered at ca. 520 nm with the concomitant appearance of a new band at ~660 nm. However, in the last part of the titration a decrease of this red-shifted band that was followed by the appearance of a more prominent band at 544 nm and a small hypsochromic shift of the initial Soret band (ca. 4 nm) were observed. These final spectral changes can be attributed to the formation of the copper(II) complex. The formation of a well-defined isosbestic point at 530 nm is in accordance with the presence of two species in solution, corresponding to the free ligand and to the metal complex. These changes in the ground state are exemplified in Figure 3C for compound **4d**.

Considering the emission spectra, the addition of Cu^{2+} is responsible for the quenching of ca. 99% in the two bands centered at ca. 660 and 719 nm as is exemplified in Figure 3D for compound **4d**. This behavior can be justified by nonradiative deactivation processes due to the Cu^{2+} heavy metal effect. This phenomenon is particularly favored in the presence of paramagnetic metals.³⁶ Therefore, compounds **4a–d** exhibit fluorescence quenching upon the binding of the Cu^{2+} ion typical of on–off type fluoroionophoric probes. The stability constants for the interaction of compounds **4a–d** with Cu^{2+} were also determined and are summarized in Table 3, maintaining the stoichiometry observed for the other metals.

MALDI-TOF-MS and Solid Support Studies. Since the pyrazole–porphyrin conjugates **4a–d** revealed promising ability for the detection of metal ions in solution, we decided also to study their ability as metal ion chemosensors in gas phase and in solid state supports. The interaction of conjugates **4a**, as representatives of ligands **4a–c**, and **4d**, as molecular probes in gas phase, was studied by MALDI-TOF-MS in the presence of Cu^{2+} , Zn^{2+} , Cd^{2+} , Ag^+ , and Hg^{2+} ions using molar ratios of metal/ligand of 2:1, 1:1, and 1:2. The ligands were dissolved in chloroform and the metal salts in acetonitrile as previously described. The metal ion titrations were performed using the dried-droplet approach and layer-by-layer deposition (see Experimental Section). In both methods, the pyrazole–porphyrin conjugates act as an internal matrix.

In the titrations with Cu^{2+} as exemplified in Figure 4 for compound **4d**, the peak at $m/z = 833.1$ was unambiguously identified as corresponding to the free base molecular ion $[\text{L}]^{+\bullet}$. After the addition of 0.5 equiv of Cu^{2+} , the peak at 893.8 m/z with 100% of intensity was identified as being due to the mononuclear species $[(4\text{d}-2\text{H})+\text{Cu}(\text{II})]^{+\bullet}$. A second peak at m/z 956.7 whose intensity increases with the ratio metal/ligand was attributed to the dinuclear species $[(4\text{d}-2\text{H})+2\text{Cu}(\text{II})]^{+\bullet}$. The peak assigned to the free-base ligand disappears after the addition of 1 equiv of Cu^{2+} when the layer-by-layer deposition method was used and after the addition of 2 equiv when the dried-droplet approach was used (see Figure 4). The titrations with Ag^+ shows behavior similar to the one described for Cu^{2+} , but the peaks detected at 940 and 1048 m/z were assigned to the mono- and dinuclear species $[\text{4d}+\text{Ag}(\text{I})]^{+\bullet}$ and $[\text{4d}+2\text{Ag}(\text{I})]^{+\bullet}$, respectively; in these cases, the ligands maintained the nitrogen inner protons.

In the others metal titrations, peaks corresponding to the mononuclear species $[\text{L}+\text{M}]^{+\bullet}$ but with low intensity were detected. In some cases, as in the titration of compound **4d** with Hg^{2+} by dried-droplet deposition only the peak assignable to the protonated ligand was detected (see Table S1,

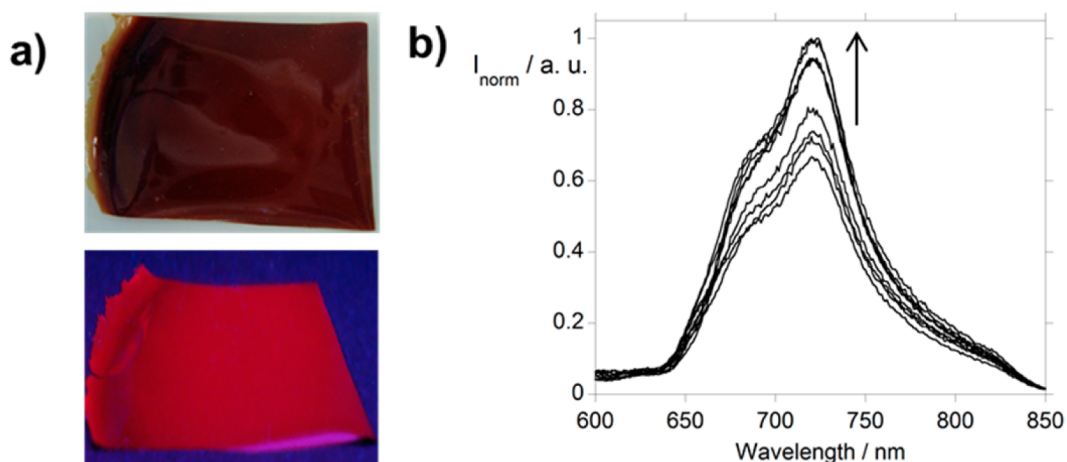


Figure 5. (a) Physical appearance of a PMMA film doped with compound **4a** at visible light (top row) and under an UV lamp ($\lambda = 365$ nm) (bottom row). (b) Emission spectra of the PMMA doped film with compound **4a** and after immersion in aqueous Zn^{2+} . (Dried films after 1, 4, 9, 14, 19, 24, 29, and 24 min, $[\text{Zn}^{2+}] = 1.0 \times 10^{-3}$ M, and $\lambda_{\text{exc4a}} = 539$ nm.)

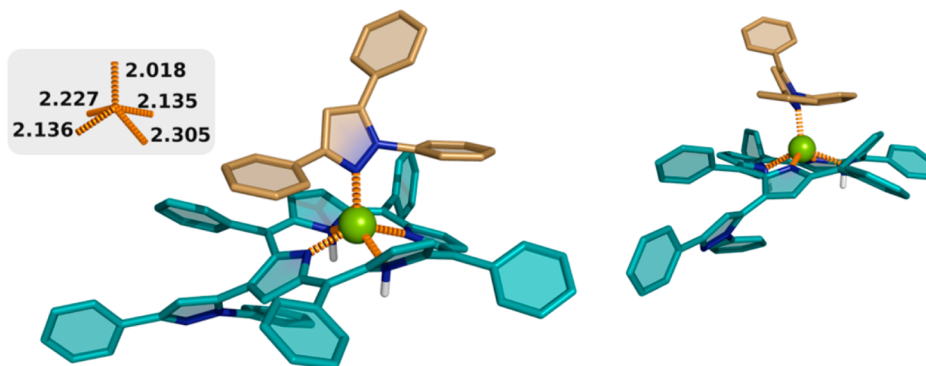


Figure 6. Two views of the 1:2 (M/L) complex involving Zn^{2+} and **4a**, in which one of the ligands has been replaced by a **4a**-like replacement (see main text for additional details), as calculated at the B3LYP/LanL2DZ level. The inset highlights the $\text{N} \cdots \text{Zn}^{2+}$ distances in the same orientation as the complex. Color code: teal/beige, carbon; green, zinc; blue, nitrogen; white, hydrogen (noninteracting hydrogens have been omitted for the sake of clarity).

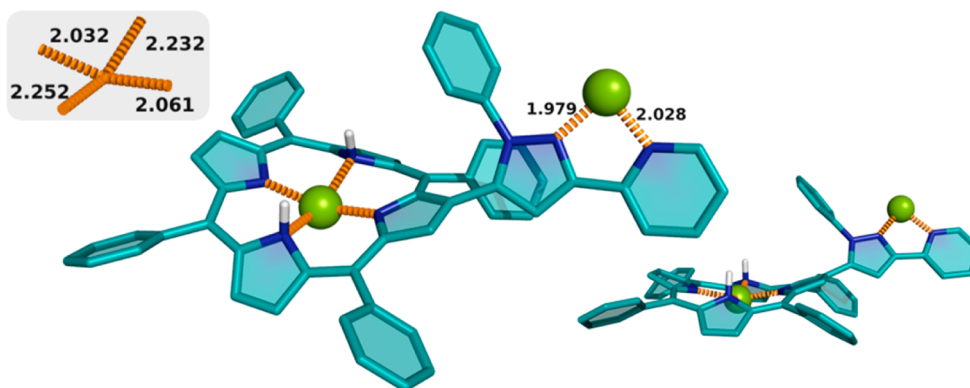


Figure 7. Two views of the 2:1 (M/L) complex involving Zn^{2+} and **4d**, as calculated at the B3LYP/LanL2DZ level. The remaining details are as described in Figure 6.

Supporting Information). These results suggest the instability of the complexes formed when the titrations were performed using the same stoichiometric metal/ligand amounts.

The MALDI-TOF-MS studies suggest that ligands based on pyrazole-porphyrin conjugates **4a–d** can be used to sense metal ions in gas phase with high selectivity toward Cu^{2+} and Ag^+ .

Considering the possibility of constructing a real solid sensor based on the reported compounds, we prepared thin films using the low cost polymer poly(methyl methacrylate) (PMMA) and ligand **4a**, in the absence of water. The fluorescence emission properties of the polymer doped with the selected conjugate were explored using an optical fiber device connected to the spectrofluorimeter. The strategy is very simple and is commonly applied to emissive lanthanide complexes that

increase the luminescence and brightness in the absence of water.³⁷

The PMMA doped films were immersed in an 1.0×10^{-3} M aqueous solution of Zn^{2+} , Cu^{2+} , Cd^{2+} , Ag^{+} , or Hg^{2+} at room temperature and dried with air. The emission intensity was measured after each spraying. In Figure 5 is represented the variation in the fluorescence intensity of PMMA film doped with conjugate **4a** in the presence of aqueous Zn^{2+} . It clearly shows an interaction with the ligand, and as a consequence, the fluorescence emission with a maximum at 719 nm was enhanced over time.

When the PMMA doped films were sprayed with aqueous solutions of others metal ions under study (Cu^{2+} , Cd^{2+} , Hg^{2+} , or Ag^{+}), no variation in the fluorescence intensity were observed. These preliminary results show clearly a promising application of pyrazole–porphyrin conjugates in the PMMA polymer as a new solid supported metal chemosensor to detect Zn^{2+} in water.

Theoretical Calculations. The conformational aspects pertaining to the complexation of **4a** and **4d** to the metal cations in their experimentally determined 2:1 and 1:2 (metal-to-ligand) stoichiometries, respectively, were studied through density functional theory (DFT) calculations. The Zn^{2+} complexes were chosen as being representative of the remaining binding arrangements. In the case of **4d**, where two ligand molecules bind to a single metal cation, one of the ligand molecules was replaced by a model ligand to reduce conformational degrees of freedom while still being representative of the entire complex, particularly the interaction of the pyrazole fragment with the cation and the porphyrinic core of the other ligand.

In Figure 6 is shown the lowest energy conformation of the complex formed by one **4a** ligand, one **4a**-like ligand, and a single Zn^{2+} cation, modeling the 1:2 (M/L) complex. The cation sits inside the porphyrinic core, slightly above the plane defined by the four core nitrogens, coordinating to the porphyrin nitrogens with $N_{\text{porphyrin}} \cdots \text{Zn}^{2+}$ distances ranging from 2.14 to 2.31 Å. The pyrazole fragment from the other ligand hovers over the porphyrinic core of the first ligand, allowing the establishment of a shorter $N_{\text{pyrazol}} \cdots \text{Zn}^{2+}$ interaction with length 2.02 Å. The two phenyl fragments attached to the pyrazole ring are almost coplanar with the porphyrin core of the other ligand, suggesting the possibility of $\pi \cdots \pi$ interactions between both aromatic systems. The entire binding arrangement leads to a coordination sphere resembling a square-based pyramid.

In the 2:1 (M/L) complexation involving ligand **4d** (Figure 7), one of the metals sits, similarly to that in the complex with **4a**, inside the porphyrinic core, just slightly above the plane defined by the four nitrogens. In this case, the $N_{\text{porphyrin}} \cdots \text{Zn}^{2+}$ distances are slightly shorter, ranging from 2.03 to 2.25 Å; the two inner-core protons point outside the ring, opposite the cation, thus minimizing the electrostatic repulsion between themselves and the cation. The two $N_{\text{porphyrin}} \cdots \text{Zn}^{2+}$ distances involving the protonated nitrogens are ca. 0.1 to 0.2 Å longer than the remaining two (a similar result is encountered in the complex involving **4a**). The second Zn^{2+} cation coordinates to the pyrazole fragment through the chelate pyrazole and pyridine nitrogens, leading to the $N \cdots \text{Zn}^{2+}$ distances of 1.98 and 2.03 Å.

CONCLUSIONS

In this work, an efficient access to prepare the new pyrazole–porphyrin conjugates **4a–d** that use the tetrapyrrolic core and the pyrazole moiety as the signaling fluorophore and as metal ion receptor was developed. The binding of these new conjugates with Zn^{2+} induces significant changes in the ground state and in the ratio of the fluorescence peaks typical from a ratiometric-type fluoroionophoric probe. Upon their binding with Cu^{2+} , pyrazole–porphyrin ligands present a quenching of the emission intensity characteristic of an on–off type fluoroionophoric probe. When the ability of these conjugates in the detection of metal ions in gas phase is combined to their immobilization in PMMA films, pyrazole–porphyrin conjugates emerge as versatile porphyrin-based molecular sensors.

ASSOCIATED CONTENT

Supporting Information

Full nuclear magnetic resonance data for all new compounds and additional photophysical characterization of compounds **4a**, **4c**, and **4d**, and major peaks observed in the metal titration of chemosensor **4d**. This material is available free of charge via the Internet at <http://pubs.acs.org>.

AUTHOR INFORMATION

Corresponding Authors

*(M.G.P.M.S.N.) Tel: +351 234370710. Fax: +351 234370084.

E-mail: gneves@ua.pt.

*(C.L.) Tel: +351 212948300. Fax: +351 212948550. E-mail: cle@fct.unl.pt.

Notes

The authors declare no competing financial interest.

ACKNOWLEDGMENTS

We are grateful to the Universidade de Aveiro, Fundação para a Ciência e a Tecnologia (FCT), European Union, QREN, FEDER, and COMPETE for funding the QOPNA research unit (project PEst-C/UI0062/2013). We acknowledge the Portuguese National NMR Network (RNRMN), supported by funds from FCT, Scientific PROTEOMASS Association (Portugal), and REQUIMTE (PEst-C/EQB/La0006/2013) for general funding. N.M.M.M. and S.M.S. thank FCT/MEC for their Post-Doctoral Grants SFRH/BPD/84216/2012 and SFRH/BPD/64752/2009. C.N. thanks the Xunta de Galicia (Spain) for her postdoctoral contract (I2C program).

REFERENCES

- (1) (a) Beer, P. D.; Gale, P. A. *Angew. Chem., Int. Ed.* **2001**, *40*, 486. (b) Martínez-Máñez, R.; Sancenón, F. *Chem. Rev.* **2003**, *103*, 4419. (c) Wang, B.; Anslyn, E. V. *Chemosensors: Principles, Strategies and Applications*; John Wiley & Sons, Inc.: Singapore, 2011.
- (2) (a) Bühlmann, P.; Pretsch, E.; Bakker, E. *Chem. Rev.* **1998**, *98*, 1593. (b) Fan, L.-J.; Zhang, Y.; Murphy, C. B.; Angell, S. E.; Parker, M. F. L.; Flynn, B. R.; Jones, W. E., Jr. *Coord. Chem. Rev.* **2009**, *253*, 410.
- (3) Rogers, C. W.; Wolf, M. O. *Coord. Chem. Rev.* **2002**, *233–234*, 341.
- (4) (a) Prodi, L.; Bolletta, F.; Montalti, M.; Zaccaroni, N. *Coord. Chem. Rev.* **2000**, *205*, 59. (b) Lodeiro, C.; Capelo, J. L.; Mejuto, J. C.; Oliveira, E.; Santos, H. M.; Pedras, B.; Nuñez, C. *Chem. Soc. Rev.* **2010**, *39*, 2948.
- (5) Kim, J. S.M.; Quang, D. T. *Chem. Rev.* **2007**, *107*, 3780.
- (6) Kimura, E.; Koike, T. *Chem. Soc. Rev.* **1998**, *27*, 179.
- (7) (a) Li, Y.; Shao, J.; Yu, X.; Xu, X. *J. Fluoresc.* **2010**, *20*, 3. (b) Yang, Z.; Zhang, K.; Gong, F.; Li, S.; Chen, J.; Ma, J. S.; Sobenina,

- L. N.; Mikhaleva, A. I.; Trofimov, B. A.; Yang, G. J. *Photochem. Photobiol. A* **2011**, 217, 29.
- (8) (a) Guerrero, M.; Pons, J.; Font-Bardia, M.; Calvet, T.; Ros, J. *Aust. J. Chem.* **2010**, 63, 958. (b) Elanchezian, V. S.; Kandaswamy, M. *Inorg. Chem. Commun.* **2010**, 13, 1109. (c) Ciupa, A.; Mahon, M. F.; De Bank, P. A.; Caggiano, L. *Org. Biomol. Chem.* **2012**, 10, 8753.
- (9) Burdette, S. C.; Walkup, G. K.; Spingler, B.; Tsien, R. Y.; Lippard, S. J. *J. Am. Chem. Soc.* **2001**, 123, 7831.
- (10) (a) Xu, A.; Baek, K.-H.; Kim, H. N.; Cui, J.; Qian, X.; Spring, D. R.; Shin, I.; Yoon, J. *J. Am. Chem. Soc.* **2010**, 132, 601. (b) Xu, Z.; Yoon, J.; Spring, R. *Chem. Soc. Rev.* **2010**, 39, 1996.
- (11) (a) Ratte, H. T. *Environ. Toxicol. Chem.* **1999**, 18, 89. (b) Lin, Y.-H.; Tseng, W. L. *Chem. Commun.* **2009**, 6619. (c) Li, H.; Zhai, J.; Sun, X. *Langmuir* **2011**, 27, 4305. (d) El-Safty, S. A.; Khairy, M.; Ismael, M. *Sensor Actuators, B* **2012**, 166–167, 253. (e) Li, Y.; Li, L.; Pu, X.; Ma, G.; Wang, E.; Kong, J.; Liu, Z. *Bioorg. Med. Chem. Lett.* **2012**, 22, 4014. (f) Yuan, M.; Zhu, Y.; Lou, X.; Chen, C.; Wei, G.; Lan, M.; Zhao, J. *Biosens. Bioelectron.* **2012**, 31, 330.
- (12) Boening, D. W. *Chemosphere* **2000**, 40, 1335.
- (13) (a) Okamoto, K.; Fukuzumi, S. *J. Am. Chem. Soc.* **2004**, 126, 13922. (b) Weng, Y.-Q.; Yue, F.; Zhong, Y.-R.; Ye, B.-H. *Inorg. Chem.* **2007**, 46, 7749. (c) Zhang, J. F.; Zhou, Y.; Yoon, J.; Kim, Y.; Kim, S. J.; Kim, J. S. *Org. Lett.* **2010**, 12, 3852.
- (14) Rambo, B. M.; Sessler, J. L. *Chem.—Eur. J.* **2011**, 17, 4946.
- (15) (a) Chan, W. H.; Yang, R. H.; Wang, K. M. *Anal. Chim. Acta* **2001**, 444, 261. (b) Luo, H.-Y.; Jiang, J.-H.; Zhang, X.-B.; Li, C.-Y.; Shen, G.-L.; Yu, R.-Q. *Talanta* **2007**, 72, 575. (c) Han, Z.-X.; Luo, H.-Y.; Zhang, X.-B.; Kong, R.-M.; Shen, G.-L.; Yu, R.-Q. *Spectrochim. Acta, Part A* **2009**, 72, 1084. (d) Bunttem, R.; Intasiri, A.; Luengchaichawewn, W. J. *Colloid Interface Sci.* **2010**, 347, 8. (e) Chen, Y.; Jiang, J. *Org. Biomol. Chem.* **2012**, 10, 4782.
- (16) (a) Kim, H. N.; Ren, W. X.; Kim, J. S.; Yoon, J. *Chem. Soc. Rev.* **2012**, 41, 3210. (b) Luo, H.-Y.; Zhang, X.-B.; Jiang, J.-H.; Li, C.-Y.; Peng, J.; Shen, G.-L.; Yu, R.-Q. *Anal. Sci.* **2007**, 23, 551.
- (17) Elguero, J. In *Comprehensive Heterocyclic Chemistry*; Katritzky, A. R., Rees, C. W., Scriven, E. F. V., Eds.; Pergamon: Oxford, 1996; Vol. 5.
- (18) Willy, B.; Müller, T. J. *J. Eur. J. Org. Chem.* **2008**, 4157.
- (19) Moura, N. M. M.; Faustino, M. A. F.; Neves, M. G. P. M. S.; Tomé, A. C.; Rakib, E. M.; Hannioui, A.; Mojahidi, S.; Hackbarth, S.; Röder, B.; Paz, F. A. A.; Silva, A. M. S.; Cavaleiro, J. A. S. *Tetrahedron* **2012**, 68, 8181.
- (20) Cavaleiro, J. A. S.; Tomé, A. C.; Neves, M. G. P. M. S. In *Handbook of Porphyrin Science*; Kadish, K. M., Smith, K. M., Guillard, R., Eds.; World Scientific Publishing Co.: Singapore, 2010; Vol. 2, p 193.
- (21) (a) Faustino, M. A. F.; Neves, M. G. P. M. S.; Vicente, M. G. H.; Silva, A. M. S.; Cavaleiro, J. A. S. *Tetrahedron Lett.* **1996**, 37, 3569. (b) Silva, A. M. G.; Faustino, M. A. F.; Tomé, A. C.; Neves, M. G. P. M. S.; Silva, A. M. S.; Cavaleiro, J. A. S. *J. Chem. Soc., Perkin Trans. 1* **2001**, 2572. (c) Silva, E. M. P.; Giuntini, F.; Faustino, M. A. F.; Tomé, J. P. C.; Neves, M. G. P.; Tomé, A. C.; Silva, A. M. S.; Santana-Marques, M. G.; Ferrer-Correia, A.; Cavaleiro, J. A. S.; Caeiro, M. F.; Duarte, R. R.; Tavares, S. A. P.; Pegado, I. N.; d'Almeida, B.; De Matos, A. P. A.; Valdeira, M. L. *Bioorg. Med. Chem. Lett.* **2005**, 15, 3333. (d) Silva, A. M. G.; Lacerda, P. S. S.; Tomé, A. C.; Neves, M. G. P. M. S.; Silva, A. M. S.; Cavaleiro, J. A. S.; Marakova, E. A.; Lukyanets, E. A. *J. Org. Chem.* **2006**, 71, 8352. (e) Silva, A. M. G.; de Oliveira, K. T.; Faustino, M. A. F.; Neves, M. G. P.; Tomé, A. C.; Silva, A. M. S.; Cavaleiro, J. A. S.; Brandão, P.; Felix, V. *Eur. J. Org. Chem.* **2008**, 704.
- (22) (a) Chimenti, F.; Bizzarri, B.; Manna, F.; Bolasco, A.; Secci, D.; Chimenti, P.; Granese, A.; Rivanera, D.; Lilli, D.; Scaltrito, M. M.; Brenciaglia, M. I. *Bioorg. Med. Chem. Lett.* **2005**, 15, 603. (b) Outirite, M.; Lebrini, M.; Lagrenée, M.; Bentiss, F. *J. Heterocyclic Chem.* **2008**, 45, 503. (c) Sun, Y.-F.; Cui, Y.-P. *Dyes Pigments* **2009**, 81, 27. (d) Bonesi, M.; Loizzo, M. R.; Statti, G. A.; Michel, S.; Tillequin, F.; Menichini, F. *Bioorg. Med. Chem. Lett.* **2010**, 20, 1990. (e) Insuasty, B.; Tigreros, A.; Orozco, F.; Quiroga, J.; Abonía, R.; Noguera, M.; Sanchez, A.; Cobo, J. *Bioorg. Med. Chem.* **2010**, 18, 4965.
- (23) Armarego, W. L. F.; Perrin, D. D. In *Purification of Laboratory Chemicals*, 4th ed.; Butterworth-Heinemann: Oxford, 1996.
- (24) Moura, N. M. M.; Faustino, M. A. F.; Neves, M. G. P. M. S.; Duarte, A. C.; Cavaleiro, J. A. S. *J. Porphyrins Phthalocyanines* **2011**, 15, 652.
- (25) Moura, N. M. M.; Faustino, M. A. F.; Neves, M. G. P. M. S.; Paz, F. A. A.; Silva, A. M. S.; Tomé, A. C.; Cavaleiro, J. A. S. *Chem. Commun.* **2012**, 48, 6142–6144.
- (26) (a) Berlman, I. B. In *Handbook of Fluorescence Spectra of Aromatic Molecules*, 2nd ed.; Academic Press: New York, 1971. (b) Montalti, M.; Credi, A.; Prodi, L.; Gandolfi, M. T. In *Handbook of Photochemistry*, 3rd ed.; Taylor & Francis: Boca Raton, FL, 2006.
- (27) Raj, D. B. A.; Francis, B.; Reddy, M. L. P.; Batorac, R. R.; Lynch, V. M.; Cowley, A. H. *Inorg. Chem.* **2010**, 49, 9055.
- (28) Moudam, O.; Rowan, B. C.; Alamiry, M.; Richardson, P.; Richards, B. S.; Jones, A. C.; Robertson, N. *Chem. Commun.* **2009**, 6649.
- (29) Frisch, M. J.; Trucks, G. W.; Schlegel, H. B.; Scuseria, G. E.; Robb, M. A.; Cheeseman, J. R.; Scalmani, G.; Barone, V.; Mennucci, B.; Petersson, G. A.; Nakatsuji, H.; Caricato, M.; Li, X.; Hratchian, H. P.; Izmaylov, A. F.; Bloino, J.; Zheng, G.; Sonnenberg, J. L.; Hada, M.; Ehara, M.; Toyota, K.; Fukuda, R.; Hasegawa, J.; Ishida, M.; Nakajima, T.; Honda, Y.; Kitao, O.; Nakai, H.; Vreven, T.; Montgomery, J. A., Jr.; Peralta, J. E.; Ogliaro, F.; Bearpark, M.; Heyd, J. J.; Brothers, E.; Kudin, K. N.; Staroverov, V. N.; Kobayashi, R.; Normand, J.; Raghavachari, K.; Rendell, A.; Burant, J. C.; Iyengar, S. S.; Tomasi, J.; Cossi, M.; Rega, N.; Millam, J. M.; Klene, M.; Knox, J. E.; Cross, J. B.; Bakken, V.; Adamo, C.; Jaramillo, J.; Gomperts, R.; Stratmann, R. E.; Yazyev, O.; Austin, A. J.; Cammi, R.; Pomelli, C.; Ochterski, J. W.; Martin, R. L.; Morokuma, K.; Zakrzewski, V. G.; Voth, G. A.; Salvador, P.; Dannenberg, J. J.; Dapprich, S.; Daniels, A. D.; Farkas, Ö.; Foresman, J. B.; Ortiz, J. V.; Cioslowski, J.; Fox, D. J. *Gaussian 09*, revision A.02; Gaussian, Inc.: Wallingford CT, 2009.
- (30) Giuntini, F.; Faustino, M. A. F.; Neves, M. G. P. M. S.; Tomé, A. C.; Silva, A. M. S.; Cavaleiro, J. A. S. *Tetrahedron* **2005**, 61, 10454.
- (31) Buchler, J. W. In *Porphyrins and Metalloporphyrins*; Smith, K. M., Ed.; Elsevier: Amsterdam, 1975; Chapter 5, p 157.
- (32) Rohatgi-Mukherjee, K. K. *Fundamentals of Photochemistry*; Wiley Eastern Limited: Calcutta, 1992.
- (33) (a) Srinivasan, A.; Kumar, M. R.; Pandian, R. P.; Mahajan, S.; Pushpan, S.; Sridevi, B.; Narayanan, S. J.; Chandrashekar, T. K. *J. Porphyrins Phthalocyanines* **1998**, 2, 305. (b) Liu, Z.-B.; Zhu, Y.; Zhu, Y.-Z.; Tian, J.-G.; Zheng, J.-Y. *J. Phys. Chem. B* **2007**, 111, 14136.
- (34) Gans, P.; Sabatini, A.; Vacca, A. *Talanta* **1996**, 43, 1739.
- (35) McClure, D. S. *J. Chem. Phys.* **1952**, 20, 682.
- (36) Formica, M.; Fusi, V.; Giorgi, L.; Micheloni, M. *Coord. Chem. Rev.* **2012**, 256, 170.
- (37) (a) McGehee, M. D.; Bergstedt, T.; Zhang, C.; Saab, A. P.; O'Regan, M. B.; Bazan, G. C.; Srdanov, V. I.; Heeger, A. J. *Adv. Mater.* **1999**, 11, 1349. (b) Balamurugan, A.; Reddy, M. L. P.; Jayakannan, M. *J. Phys. Chem. B* **2009**, 113, 14128. (c) Boyer, J. C.; Johnson, N. J. J.; van Veggel, F. C. J. M. *Chem. Mater.* **2009**, 21, 2010. (d) Kai, J.; Parrab, D. F.; Brito, H. F. *J. Mater. Chem.* **2008**, 18, 4549. (e) Zhang, H.; Song, H.; Dong, B.; Han, L.; Pan, G.; Bai, X.; Fan, L.; Lu, S.; Zhao, H.; Wang, F. *J. Phys. Chem. C* **2008**, 112, 9155.